Acta Agrobotanica

Article ID: 176077
DOI: 10.5586/aa/176077

Publication History
Received: 2023-08-06
Accepted: 2023-11-29
Published: 2024-03-07

Handling Editor
Bożena Denisow; University of Life Sciences in Lublin, Lublin, Poland; https://orcid.org/0000-0001-6718-7496

Funding
This work was supported by the Ministry of Science and Higher Education of Poland as part of the statutory activities of the Department of Botany, Warsaw University of Life Sciences - SGGW.

Competing Interests
No competing interests have been declared.

Copyright Notice
© The Author(s) 2024. This is an open access article distributed under the terms of the Creative Commons Attribution License, which permits redistribution, commercial and noncommercial, provided that the article is properly cited.

ORIGINAL RESEARCH

Structure of root nodules in *Laburnum anagyroides* Medik.

Barbara Łotocka *

Department of Botany, Warsaw University of Life Sciences - SGGW, Nowoursynowska 159, 02-776, Warszawa, Poland

* To whom correspondence should be addressed. Email: kbot@sggw.edu.pl

Abstract

The structure of the *Laburnum anagyroides* root nodules was studied by means of classical light and transmission electron microscopy methods. The ability of cross-inoculation and effective nodulation by rhizobial microsymbionts, effective in other genistean species, was not confirmed in *L. anagyroides*. However, the seedlings were successfully albeit ineffectively nodulated by non-identified rhizobia from soil sampled under established *L. anagyroides* trees. The microscopic (ultra)structure of these nodules met the basic criteria of genistoid nodules: their meristem was apically positioned and contained two domains (infected and non-infected one), non-bacteroidal rhizobia persisted in apoplast enclaves, and intra-nodule rhizobial infection was passed from cell to cell by host cell division and not by infection threads. The developmental disturbances detected in the nodules (primarily, formation of multi-bacteroid sacs instead of typical single-bacteroid symbiosomes and proliferation apoplast enclaves with accompanying cell wall discontinuities) suggested that the host plant incorrectly recognized the microsymbiont used in the present study.

Keywords

bacteroid-containing tissue; Fabaceae; Genisteae; indeterminate root nodule; ineffective root nodule; nodule endodermis; root nodule meristem

1. Introduction

Laburnum sp. (Fabaceae, Faboideae, Genisteae; Stevens, 2001) is currently considered to belong to the "core" genistoid clade, tribe Genisteae (Cardoso et al., 2013), *Cytisus* group (Cristofolini & Conte, 2002). It is a deciduous woodland tree up to 7 m tall, with trifoliolate leaves, and its pendulous racemes are up to 40.0 cm long and attractive due to the abundant yellow flowers (Seneta et al., 2021). *L. anagyroides* (syn. *Cytisus laburnum* L., Eng. common laburnum, golden chain, or golden rain) is not native to Poland, as its native geographical range extends throughout the considerably warmer parts of Europe: mountain chains of central and southern Europe (the upper elevation limit ca. 1800 m), from the Jura in eastern France to the Balkan Peninsula (Cristofolini & Chiapella, 1984; Rivers, 2017). According to the data on the website of the Polish Nurserymen Association (2023), *L. anagyroides* is reproduced in over a dozen Polish nurseries by grafting cultivars on *L. anagyroides* seedlings. The status of this species in Polish flora was changed from a cultigen to a non-invasive kenophyte, as it was found to be established locally in a few natural and semi-natural communities in Western Poland (Tokarska-Guzik et al., 2012). Occasionally *L. anagyroides* is used for land rehabilitation of disturbed areas (e.g., the waste dumps of the heat and power plant Siekierki in Warszawa, Poland), but this genistean is mostly cultivated as an ornamental tree in public parks and private gardens; interestingly, many trees known to the author for over 20 years do not reach the height given as the maximum for the species. Their poor performance may be simply due to unfavorable habitat conditions, as they are urban-grown plants (Zalewska et al., 2023). The urban environment is characterized by intensified processes of xerization of climatic conditions and a strong

and diverse transformation of the abiotic environment (atmosphere, soil, water), including pollution with chemical and physical factors (Wysocki, 2019), which affects the condition of urban plants and the microbiome of urban soils. However, it is also possible that *L. anagyroides* trees lack effective symbiosis with rhizobia, and most faboids (97% of examined species) are dependent on dinitrogen fixation in root nodules (Bryan et al., 1996).

All the genistean species investigated so far by the author or described in the literature form root nodules of the indeterminate type with an apical or lateral meristem (the latter specific for *Lupinus* spp.), which has an organization unique for the tribe (review and original results: Łotocka, 2008). Namely, the meristem has two domains, infected (i.e., the meristematic cells contain symbiosomes) and non-infected ones, and the domains contribute to the formation of specific nodule tissues: the former produces cells differentiating into the centrally-located bacteroid-containing tissue (BT) functional in the dinitrogen fixation, and the latter one contributes cells for the development of apical and lateral cortical tissues and for the elongation of vascular bundles. However, there is no information on the nodule structure in *L. anagyroides* Medik. Rhizobial strains nodulating the genisteans studied so far are most often classified among 7 distinct species and numerous partially characterized strains of *Bradyrhizobium* sp., in superclades *Bradyrhizobium japonicum* or *Bradyrhizobium elkanii* (review and original results: Stępkowski et al., 2018). Although no comprehensive study is available, it is generally accepted that the particular strains accept different genistean species as the host, and therefore genistean microsymbionts form a cross-inoculation group (Kalita et al., 2006; Ruiz-Díez et al., 2009; Sajnaga et al., 2001; Stępkowski et al., 2003). This is consistent with the author's own observations that strains isolated from *Lupinus* sp. or *Sarothamnus scoparius* or *Cytisus* sp. cross-infect and effectively nodulate genisteans of other species as well (Łotocka, 2008).

Taking the above into consideration, it was decided to look for the reasons for the suboptimal performance of *L. anagyroides* in the structure of its root nodules. In this study, it was hypothesized that ***(i)*** in *L. anagyroides*, root nodules could be induced after cross-inoculation with strains isolated from other genisteans and ***(ii)*** the *L. anagyroides* nodules were of the indeterminate elongate type, typical for most species of the tribe. These hypotheses were investigated by means of the microscopic analysis of the nodule (ultra)structure using conventional methods.

2. Material and methods

2.1. Plant material and rhizobial inocula

In October, seeds of *L. anagyroides* were collected from trees growing in a few public parks in Warszawa, Poland. They were stored in a refrigerator, and in February they were prepared for germination as follows. The seeds were chemically scarified using concentrated sulfuric acid for 2 h, rinsed with cold tap water, and surface-sterilized for 20 min with 3.5% calcium hypochlorite. From this point on, they were handled in a laminar flow chamber. The seeds were rinsed repeatedly in sterile water until the hypochlorite smell was not perceivable and transferred on 0.6% agar in sterile Petri dishes. After the next 6 days, seeds that had a broken seed coat after the chemical scarification and sterilization germinated into seedlings with a root hair zone and were taken for inoculation. However, the majority of the seeds turned out to be hard; therefore, they were removed from the Petri dishes for mechanical scarification, all in aseptic conditions. The scarification was done by removal of the hilar valve using sharp-tipped forceps, and next the seeds were placed in fresh sterile Petri dishes. Thereafter, the seeds imbibed normally and produced seedlings ready for inoculation within another 5 days.

The inoculation was done using microsymbiont cultures grown in Yeast-Mannitol Broth (Vincent, 1970). Wild type bradyrhizobial strain WM9 specific for lupine, strain CYT7 isolated from *S.* (*Cytisus*) *scoparius* nodules (Sajnaga et al., 2001), and strain Jan15 isolated from *Genista tinctoria* nodules (Kalita et al., 2006) were kindly provided by Professor Wanda Małek (University Marie Curie-Skłodowska in Lublin, Poland), whereas another lupine-specific strain, USDA3045, was obtained from

Rhizobium Culture Collection (Beltsville, US). The strains were used for inoculation either separately or in a mixture. Also, a soil filtrate was used as an inoculum; it was prepared as described by Vincent (1970) from soil samples collected under three healthy ca. 15 year-old *L. anagyroides* trees originating from a commercial nursery and grown in a non-fertilized (information from the owners) private garden in Warszawa, Poland. It was not possible to check whether these trees produced root nodules. Finally, another inoculum was made from surface-sterilized and crushed root nodules collected from the test plants (Vincent, 1970). In total, seven inoculation variants were investigated, each consisting of ca. 15 plants.

Seedlings in every inoculation batch were immersed in the inoculum for ca. 15 min and transferred to pots filled with perlite, which was previously rinsed with tap water and autoclaved. The plants were grown in a vegetation chamber under 250 W sodium lamps, 400 μEs^{-1} m^{-2} (PhAR), at ca. 23 °C and 8 h dark/16 h light photoperiod. Until the 5th day after transplantation, the plants were watered only; next, they were fertilized daily with a nitrogen-free medium for hydroponics (Łotocka et al., 1995).

2.2. Sample collection and microscopy

The plants were gently removed from perlite 25 days after inoculation (dai), rinsed thoroughly, and the root nodules, if formed, were collected for microscopy in batches respective to 10 individual plants per every inoculation variant. Every batch included several root nodules with a small root fragment and/or any non-typical (spindly usually) thickenings formed within the oldest part of the tap root or on the basal parts of lateral roots. The largest nodules (up to ca. 5 mm long) were shallowly cut parallel to the surface to facilitate reagent penetration through the nodule endodermis. The samples were fixed and further processed according to a standard protocol described elsewhere (Kalita et al., 2006). Serial semi-thin sections of nodules from 10 different plants of each batch, embedded in epoxy blocks, were cut at 3 μm thickness until the central section was obtained; then, ultra-thin sections were collected and the semi-thin serial sectioning of a block was completed. Thus, every sample provided both serial sections for light microscopy and ultra-thin sections for ultrastructure examinations. As previously found by the author, the central sagittal section was optimal for anatomical analyses of the cylindrical nodules, because a single section showed the whole complexity of the nodule anatomy, from the basal connection with the root to the apical meristem. However, due to the uneven shape of the nodules obtained in the present study, it was usually impossible to section the nodules in the exact sagittal plane. The semi-thin sections were stained with toluidine blue O (Merck; O'Brien et al., 1964) or with a mixture of methylene blue (Merck) and azure A+B (Merck; Leeson & Leeson, 1970), as described earlier.

Semi-thin sections were examined with a Provis AX70 (Olympus Corporation) microscope using bright field or DIC optics, and digital images were saved as tiff files at 2776 × 2074 pixel resolution using a DP50 digital camera (Olympus Corporation) operating under AnalySIS software (SIS). Ultra-thin sections cut from the central plane of the nodules, after slot-grid mounting and standard contrasting (Kalita et al., 2006), were examined using a JEM 100C (JEOL) transmission electron microscope (TEM), and the negatives were scanned at 1200 dpi resolution using a CanoScan 9000F Mark II (Canon) flatbed scanner at 2400 dpi and saved as tiff files.

For documentation of the results, representative images were selected and enhanced using Adobe® Photoshop® CS6 Extended (Adobe Systems Inc.) software by means of non-destructive tools Layers and/or Curves. All adjustments were done on the whole area of the image except for a few negatives whose dynamic range was beyond the scanner's reproduction ability. Such negatives were scanned twice at contrasting settings, and individual images set as layers were separately enhanced as above and merged to obtain the final image using the Panorama/ Image stack tool. Figures were prepared using CorelDRAW® 2020 (Corel Corporation) software.

3. Results

All the inoculations of *L. anagyroides* seedlings with the single strain cultures or the mixed cultures of genistean microsymbionts failed: the seedlings never formed more

than a single leaf (not shown), became chlorotic soon, and died. Their root systems did not show any structures resembling root nodules. Therefore, for inoculation of one of the failed batches as well as for a new batch of seedlings, a filtrate prepared from the soil sampled under well-established *L. anagyroides* trees was used. Seedlings inoculated with the filtrate persisted (and the failed batch was rescued), but they produced only a few yellowish leaves (indicating non-effective symbiosis) and a root system with pale root nodules (not shown). The nodules had diverse shapes. Within a single root system, along with numerous non-typical root thickenings, small rounded root nodules were usually found, as well as a few that were elongate, as expected of 25 dai indeterminate nodules, but slightly crooked or irregularly shaped. After the test-inoculation with the microsymbiont isolated from the elongate nodules, the newly-grown plants were morphologically similar to the described ones. For the following analysis of the nodule microscopic structure, the observations on the largest nodules were primarily taken into consideration, as their structure was proved to be most developmentally advanced.

Generally, the anatomical structure of the *L. anagyroides* nodules included the nodule cortex, a single or once-bifurcated vascular bundle (VB) located within the cortex, and a central infected BT (Figure 1A–B). As revealed by the serial sections analysis, the latter tissue, which is a parenchyma specialized in dinitrogen fixation, was usually separated by 2–3 cell wide layers of non-infected cells into a few discontinuous lobes consisting exclusively of infected ones. In the largest nodules only, typical developmental zonation was discernible, with the apical meristem followed by the differentiating zone and the differentiated cells, the latter located basally, at the junction of the VB with the root stele (Figure 1A). The majority of the nodules were small and contained only the meristem and differentiating zone, which included several small clusters of infected cells representing the differentiating BT (Figure 1B). The nodule-like thickenings mentioned above lacked any infected cells and contained only non-specialized parenchyma and a short VB (Figure 1C).

The nodule cortex consisted of three tissues (Figure 1A–B), specifically: ***(i)*** the outer cortex built of several layers of parenchymatic vacuolated cells with intercellular spaces discernible using the light microscope (their ultrastructure is not shown), ***(ii)*** the uniseriate nodule endodermis, which in its differentiated state was built of flat cells with thickened, lamellate, and lignified cell walls devoid of plasmodesmata (Figure 1D), and ***(iii)*** the inner cortex built of parenchymatic cells characterized by the presence of lipid bodies and numerous multi-grained and rounded amyloplasts (Figure 1E). The amount of starch deposited in cortical amyloplasts increased towards the nodule base, coordinately to the differentiation stage of the adjoining BT (Figure 1A–B). The boundary layer, i.e. a layer of cells being non-turgid due to tonoplast fragmentation (a typical anatomical feature of the inner cortex in the effective nodules), did not occur in the examined samples.

The meristem was located distally and was organized into two clearly delimited domains (Figure 2A). The infected domain, distinct due to its cells being less vacuolated than in the non-infected one, produced cells added to the BT, and the non-infected domain – to the cortical tissues. The meristematic VB apices were distinct within the non-infected domain (Figure 1B). In the meristem, dividing cells were visible within both the non-infected and infected nodule domains (Figure 2A). In the dividing infected cells, the symbiosomes were segregated like the host's organelles (Figure 2C–D: ultrastructure of cytokinetic cells, located within the infected domain and at the infected/non-infected boundary, respectively). In the infected meristematic cells, most symbiosomes contained a single bacteroid (Figure 2B–D); however, in some/the same cells, more complex structures than the symbiosome were formed, with several bacteroids enclosed within a common fine-fibrillar matrix and a membrane. Such structures were named multi-bacteroid sacs (MbS) for the purposes of this study.

They usually contained small vesicles within the matrix and deposits of electron-dense substance at the inner face of the encircling membrane (Figure 3A–C). Opposing these deposits, short cisterns of rough endoplasmic reticulum (RER) often adjoined the MbS membrane in the host's cytoplasm (not shown in Figure 3, see below). Otherwise, the image of meristematic infected cells was typical, as they also contained rounded nuclei

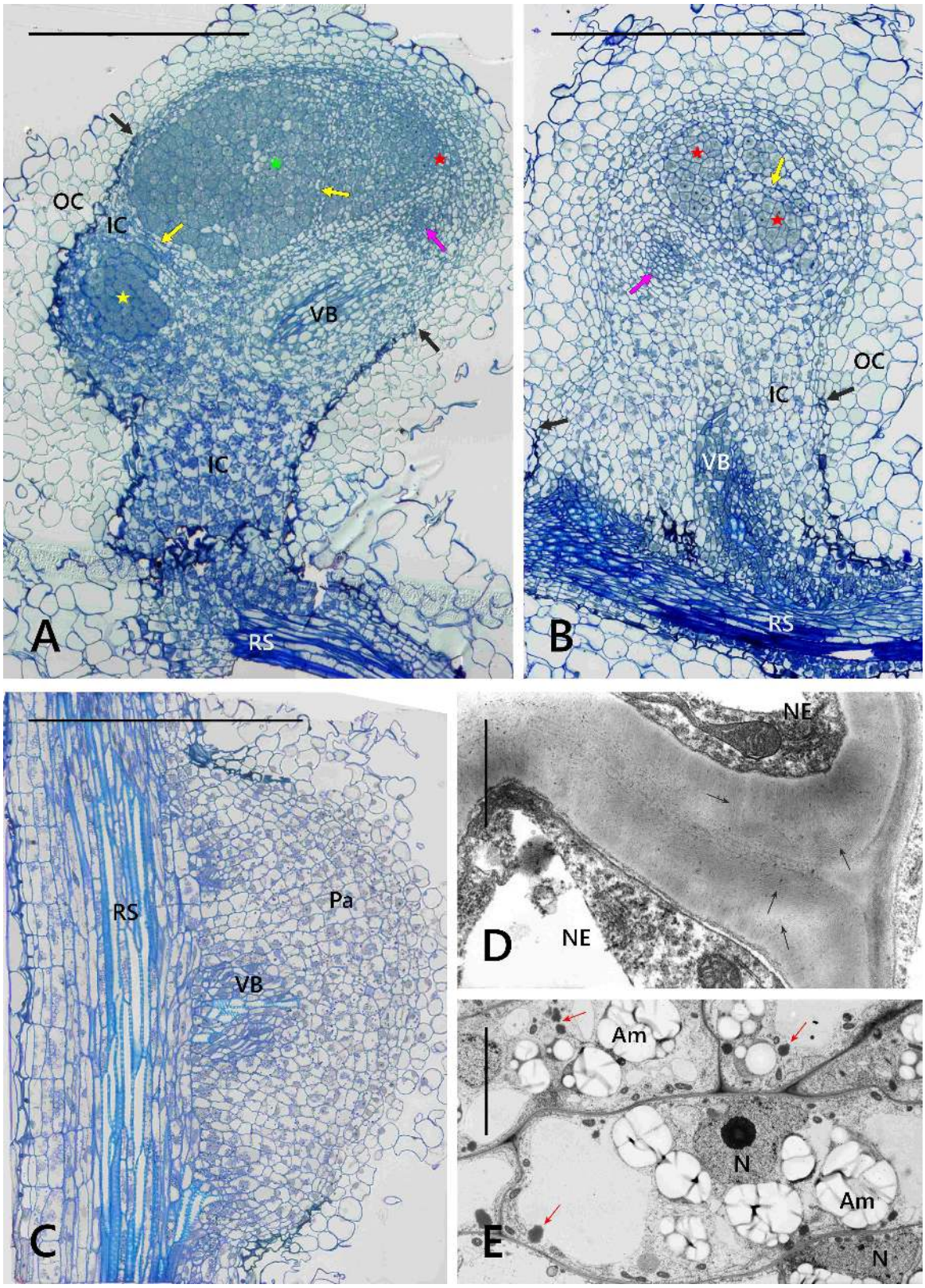

Figure 1 Nodule anatomy (**A–C**) and ultrastructure of cortical cells (**D–E**). Zonation in bacteroid-containing tissue: red asterisk - nodule meristem, green asterisk - differentiating zone, yellow asterisk - differentiated zone. Am - amyloplasts with compound starch grains; IC - nodule inner cortex; OC - nodule outer cortex; N - cell nucleus; NE - cells of nodule cortical endodermis; Pa – parenchyma; RS - root stele; pink arrow - differentiating apical part of VB; black arrows - nodule cortical endodermis, arrows are placed at its most apical differentiated cells; yellow arrow - layers of uninfected cells dissecting BT into lobes; fine black arrows - areas of striation evident in the secondary cell wall; fine red arrows - lipid bodies. Scale bars 400 µm, 400 µm, 100 µm, 1 µm, and 8 µm, respectively.

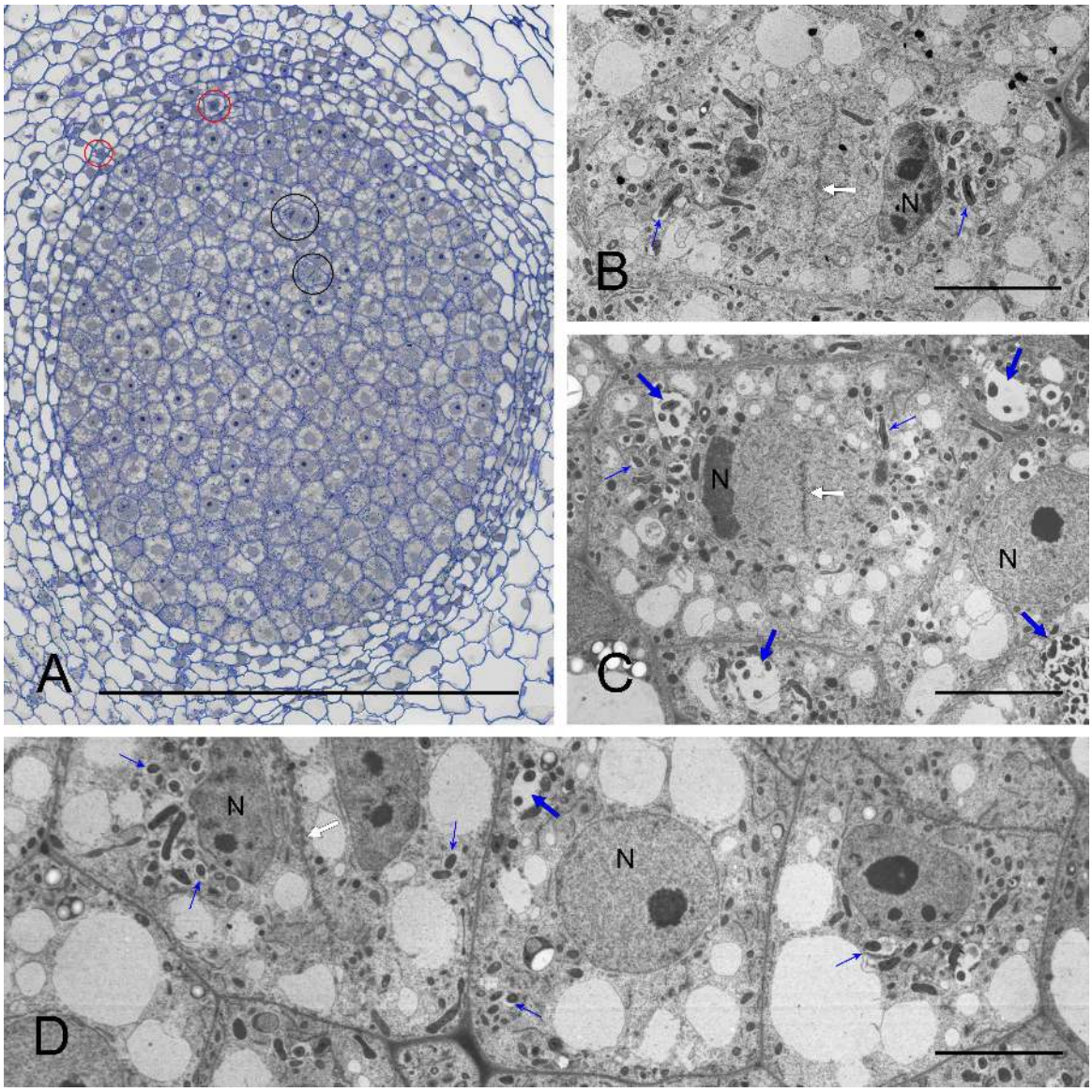

Figure 2 Nodule meristem organization (**A**) and ultrastructure (**B–D**). Note the massive, rounded infected domain surrounded by a ca. triseriate uninfected domain in (**A**), cytokineses, thin cell walls and numerous small vacuoles in the meristematic cells in (**B–D**). N - cell nucleus (reconstituting or interphasic); red circles – mitoses in the non-infected meristem domain; black circles - mitoses in the infected meristem domain; white arrows - cell plate in the cytokinetic cells; fine blue arrows - single-bacteroid symbiosomes; blue arrows - multibacteroid sacs. Scale bars 100 µm, 2 µm, 26 µm, and 42 µm, respectively.

with large nucleoli, proplastids with small starch grains, mitochondria with a distinct nucleoid-like region, numerous short RER cisterns and free ribosomes, numerous small vacuoles, and occasional dictyosomes and lipid bodies (Figure 3D).

In the differentiating BT, concurrently with the cell enlargement, the number and size of MbS increased (Figure 4A–C), but the TEM images were inconclusive whether this was attributable to the divisions of bacteroids, since the number of dividing bacteroids was generally low. The shape of the bacteroids became irregular: wavy, bumped, swollen, and/or branched (Figure 5A–D), often with an apparently fragmented nucleoid (Figure 5D). Granules of poly-beta-hydroxybutyrate became evident in their cytoplasm (Figure 5C). At the same time, the MbS matrix surrounding the bacteroids became wider and a narrow clear zone became discernible directly at the bacteroid surface. Concurrently with these changes, the host's cells enlarged. Their plastids, differentiating into amyloplasts with multiple starch grains, became elongated and were positioned along cell walls (comp. Figure 4A–C), numerous mitochondria were spatially close to them (not discernible at the magnifications in Figure 4), and the cell nucleus became irregular to lobed. The size of the amyloplasts reached

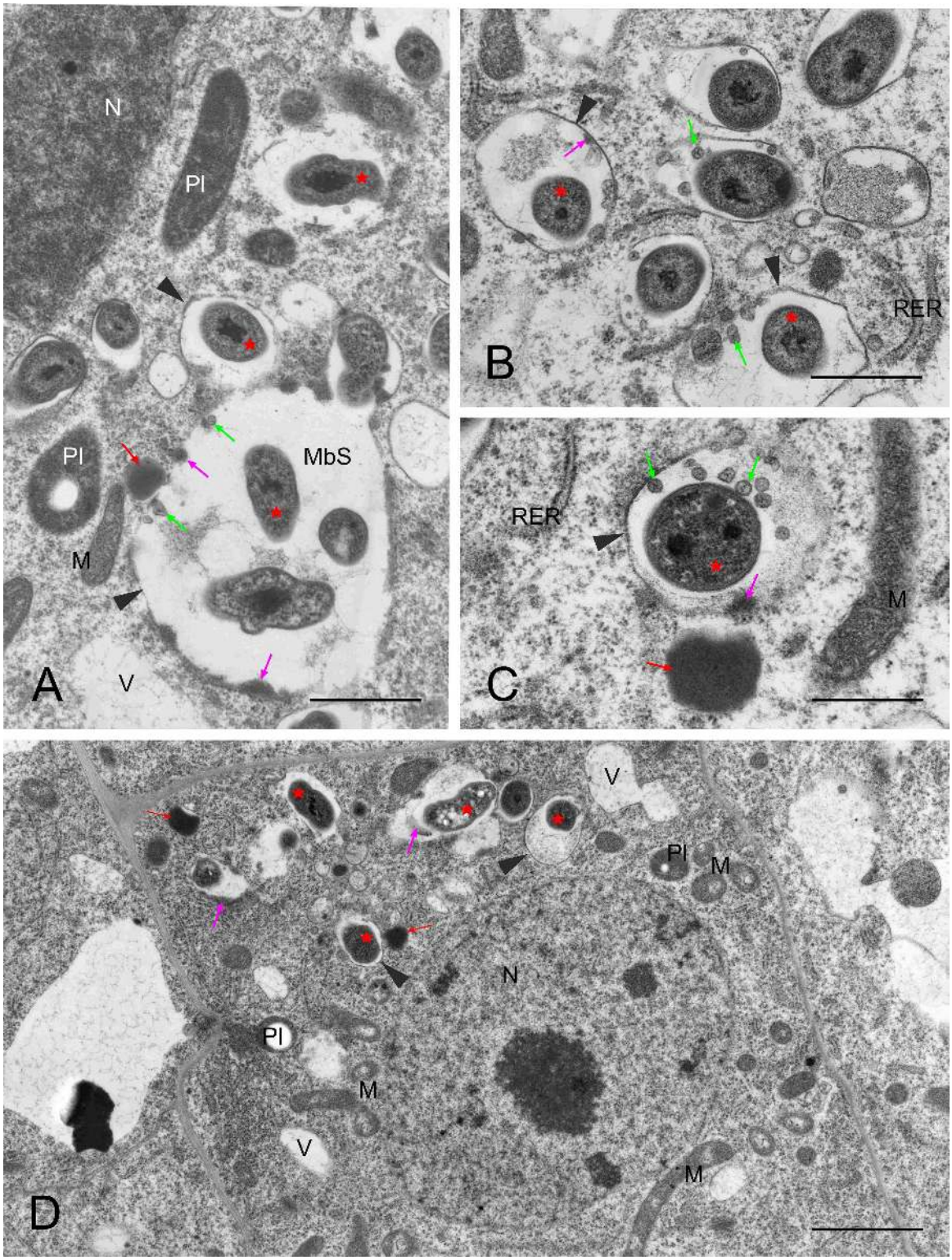

Figure 3 Ultrastructure of multibacteroid sacs (MbS, **A**) and symbiosomes (**B–D**) in the infected domain of nodule meristem. N – cell nucleus with a visible nucleolus; M – mitochondria (note the nucleoid-like region discernible in (**D**); MbS - multibacteroid sac; Pl – proplastids; RER – rough endoplasmic reticulum; fine red arrows - lipid bodies; fine green arrows – small vesicles inside symbiosomes or MbS; fine pink arrows – electron-dense substance on the inner surface of the symbiosome membranes or membranes surrounding MbS; arrowheads - symbiosome membranes or membranes surrounding MbS; red asterisks - bacteroids. Scale bars 5 µm, 1 µm, 1 µm, and 8 µm, respectively.

the maximum in the cells of starch-rich interzone II/III, i.e., in the last layer of the differentiation zone, where they were positioned preferentially at the intercellular spaces (Figure 4C).

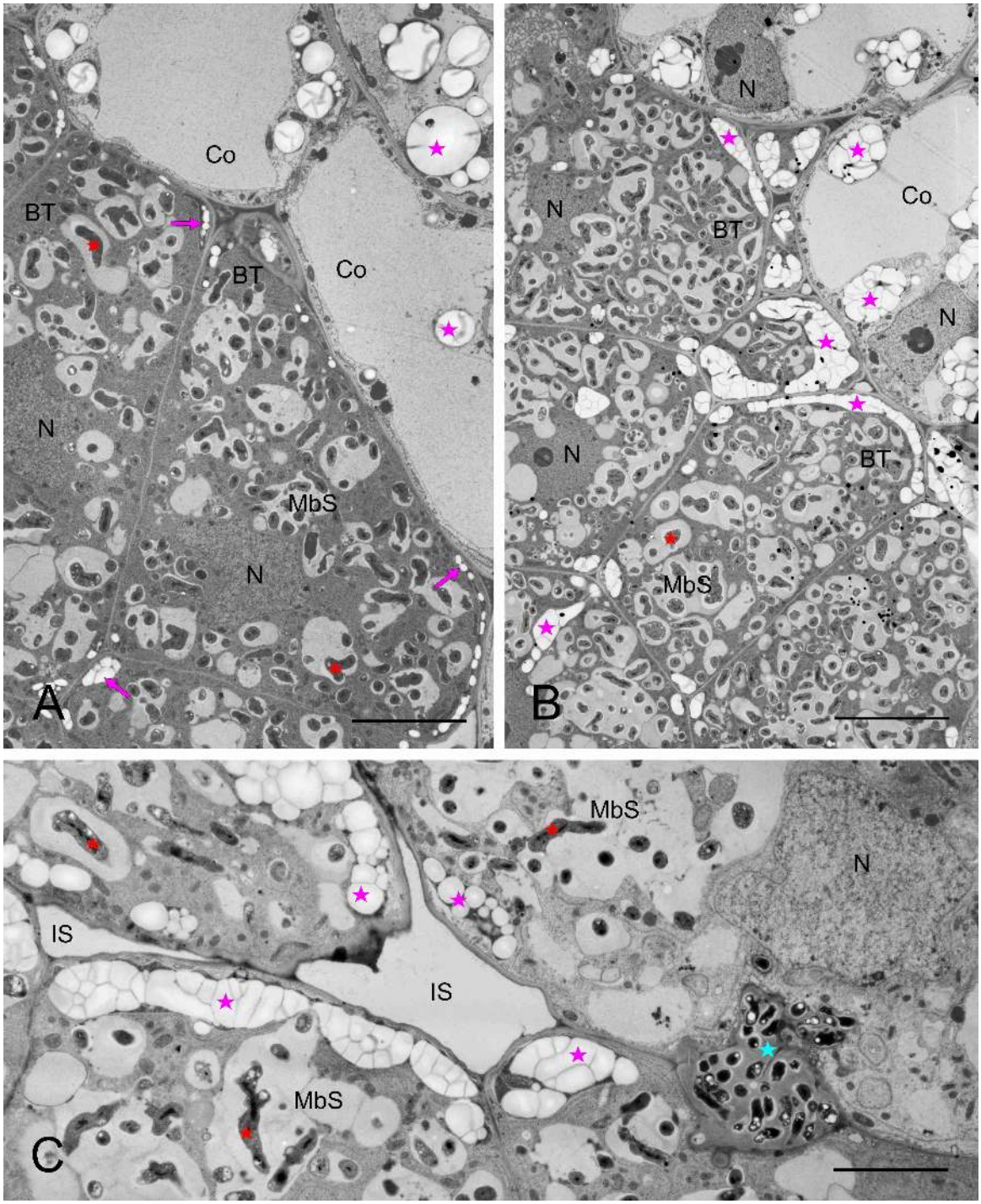

Figure 4 Ultrastructure of the differentiating bacteroid tissue: developmentally younger cells in (**A**), cells of starch-rich interzone II/III in (**B–C**), and adjoining inner cortical cells (**A–B**). BT – bacteroid tissue cells; Co – inner cortex cells; IS – intercellular spaces; MbS – mutibacteroid sacs; N – cell nuclei (note their irregular shape in the BT cells); pink asterisk or arrows – compound starch grains in amyloplasts (note the location of amyloplasts at the cell periphery in BT and the difference in the amyloplast shape between the BT and Co cells, elongated and rounded, respectively); blue asterisk – apoplast enclave enclosing multiple non-bacteroid rhizobial cells in the cell wall separating two BT cells; red asterisks – bacteroids inside the MbS. Scale bars 23 µm, 23 µm, and 32 µm, respectively.

Infection threads were never found in the nodules. Instead, the reservoir of non-bacteroidal rhizobial cells was constituted as the cell wall-associated enclaves, which are unique for genistean nodules. However, typical genistean enclaves, i.e., small and containing a single small rhizobial cell (Figure 6A) or a few of them, were infrequent. Instead, large and irregular structures were found, both using the electron (Figure 6B) and light microscopes (Figure 6C), containing multiple rhizobia of various

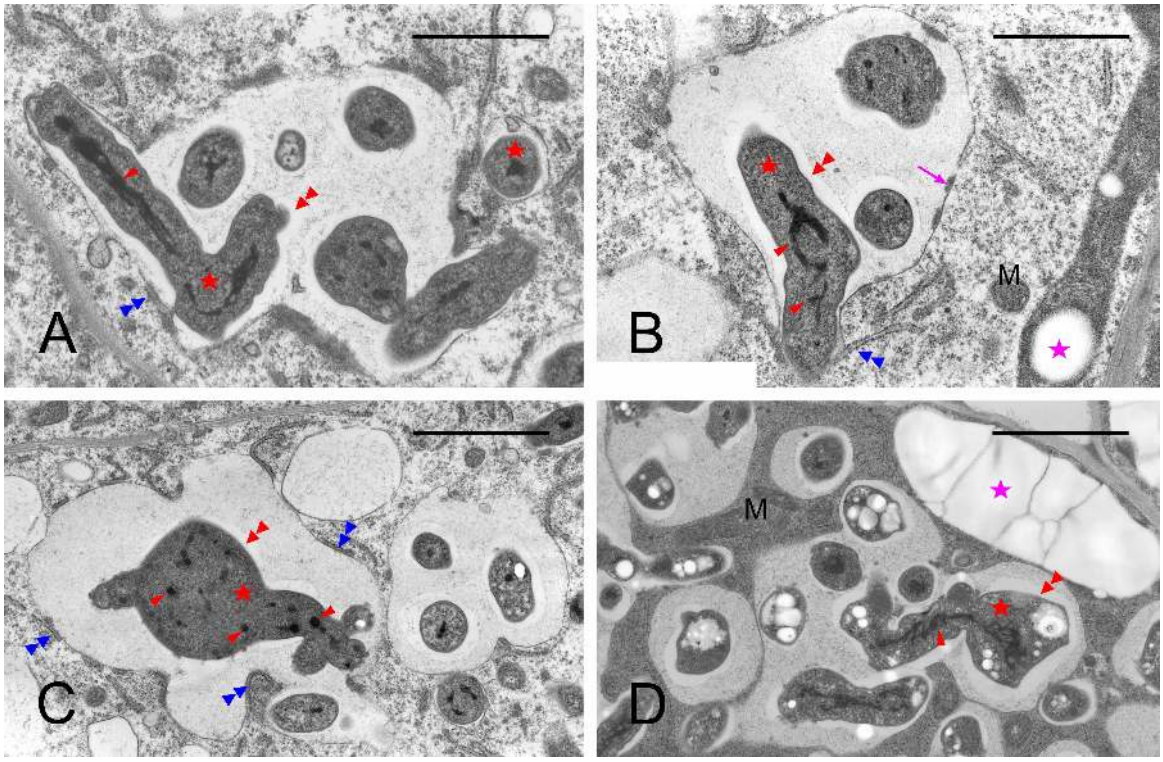

Figure 5 Ultrastructure of multibacteroid sacs (MbS) in younger differentiating BT cells (**A–C**) and in interzone II/III (**D**). M – mitochondria; red asterisks – bacteroids in MbSs (note the irregular shape of the bacteroids, the electron-transparent globules represent the poly-beta-hydroxybutyrate reserves); red arrowheads - nucleoid; double red arrowheads – light zone between the bacteroid and the MbS fibrillar matrix; fine pink arrows – electron-dense substance on the inner surface of the membranes surrounding MbS; double blue arrowheads – places of contact between RER and MbS membranes; pink asterisks – starch in plastids. Scale bars 2 µm, 2 µm, 3 µm, and 3 µm, respectively.

shapes and sizes (Figure 6B–D). In some cases, the cell wall was discontinuous in the vicinity of such an enclave, and the protoplasts of the adjoining cells were fused (Figure 6C–D). Possibly, the discontinuity accompanied all enlarged enclaves, but to prove this assumption, serial ultrathin sections would have to be examined. Apparently, rhizobia were released in the differentiated cells from some enclaves (Figure 7A) or MbS (Figure 7B), with the formation of a symbiosome containing a single bacteroid.

Within both differentiating and differentiated BT zones, individual cells or small cell clusters underwent degradation. The tonoplast was fragmented and, due to the loss of ribosomes, the cytoplasm became electron transparent (Figure 8A, differentiating zone, respectively), but the organelles were still recognizable. In the degrading differentiated cells (Figure 8B), the MbS membranes were discontinuous in places, and the bacteroids accumulated electron-dense material at the cell periphery (Figure 8B and right insert). The matrix of the wall enclaves was ultrastructurally similar as in MbS. Membrane coils and seriate membranes adjoined some bacteroids (Figure 8B inserts).

4. Discussion

Generally, in the present study, the *L. anagyroides* root nodule anatomy was consistent with the genistoid type, as described earlier for *Sarothamnus scoparius* (Sajnaga et al., 2001), *Genista tinctoria* (Kalita et al., 2006), *Ulex europaeus* and two species of *Cytisus* (Łotocka, 2008), *Lupinus luteus* (Golinowski et al., 1987), *Chamaecytisus podolicus* (Skawińska et al., 2017), and *Retama monosperma* (Selami et al., 2014). Namely, all genisteans' nodules examined to date (including the present results) were indeterminate due to the presence of a persistent meristem (apical in most species and lateral in *Lupinus* spp.) with unique organization, i.e., having two domains, an infected and uninfected one, contributing cells to different nodule tissues, and spreading of the intra-nodule rhizobial infection by host cell divisions in the infected domain. Significantly, infection threads are not formed in genistean nodules; instead, apoplas-

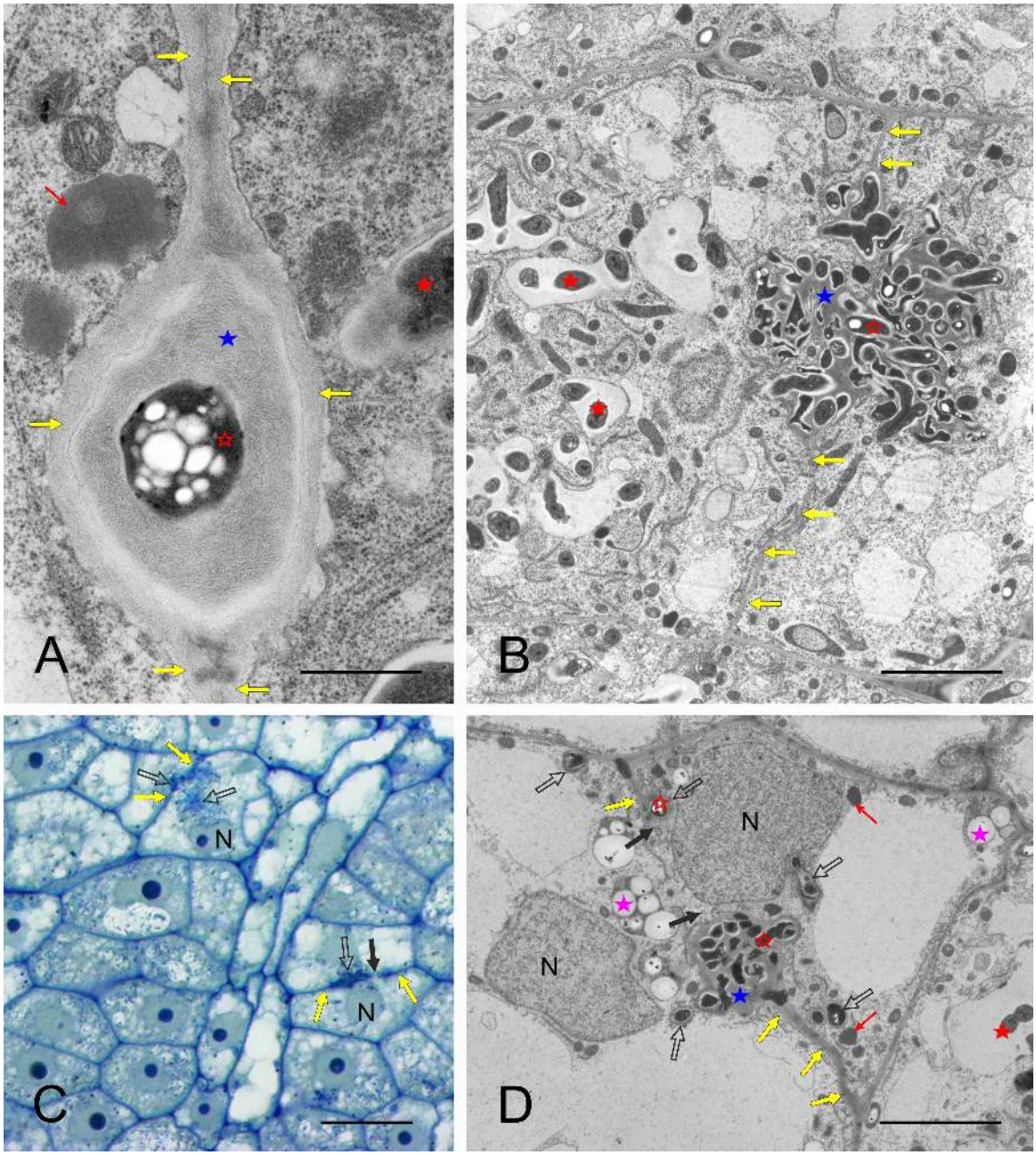

Figure 6 Ultrastructure of cell wall-associated enclaves containing non-bacteroid rhizobial cells. Single-cell enclave in (**A**) and large, branched multiple-cell enclaves in (**B–C**), note the irregular shape of rhizobial cells in (**B–D**). Discontinuities in the cell walls at the enclaves shown in (**C–D**). N – cell nucleus; yellow arrows – cell walls separating BT cells; empty black arrows – enclaves or their branches in (**D**); black arrows – discontinuity of the cell wall at the enclave; fine red arrows – lipid bodies; empty red asterisks – non-bacteroid rhizobial cells inside enclaves; red asterisks – bacteroids in MbSs; blue asterisks – enclave matrix, note its higher electron density vs. the MbS matrix; pink asterisks – starch grains. Scale bars 1 µm, 13 µm, 25 µm, and 11 µm, respectively.

tic enclaves or "arrests" constitute the refuge of non-bacteroidal rhizobia that first colonize degraded BT cells (the so-called saprotrophic zone of the nodule, Timmers et al., 2000) and ultimately return to the soil (review: Łotocka, 2008). Such enclaves were consistently found in the nodules examined in the present analysis. However, several features interpreted as developmental defects were identified in the *L. anagyroides* nodules in this study. These included the delayed development of the nodule zonation (typically, 25 day-old genistean nodules would have an already formed senescent zone, while atypically located clusters of degrading cells were found in the present analysis), a low number of nodules of a typical cylindrical shape, a pale and not pink color of the cut fresh nodules, and - considering the nodule structure – several traits implying the lack of host's balanced control on microsymbiont proliferation.

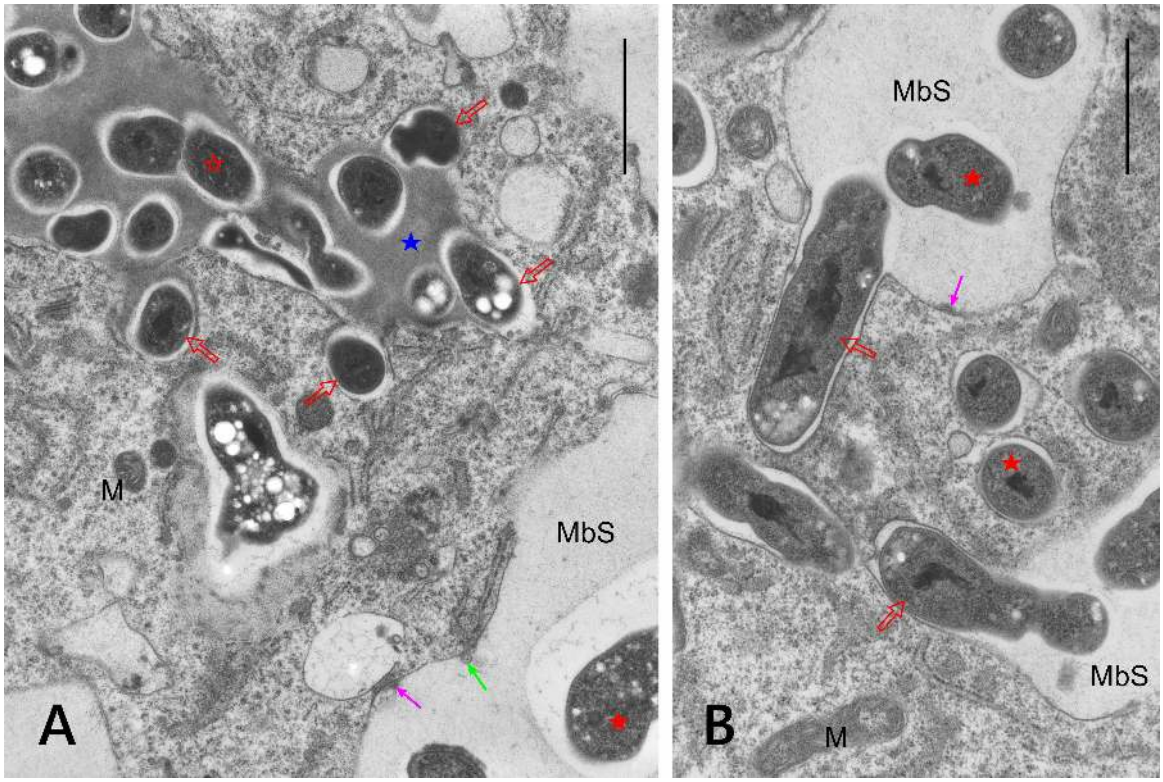

Figure 7 Ultrastructure of cell wall enclave (**A**) and MbS (**B**) with rhizobial cells or bacteroids, respectively, in peripheral positions suggesting their release with the concurrent formation of single-cell symbiosomes. M – mitochondria; MbS – multibacteroid sacs; blue asterisk – enclave matrix; empty red asterisk - non-bacteroid rhizobial cells inside enclaves; red asterisks – bacteroids in MbSs; empty red arrows – rhizobial cells or bacteroids being released from the enclave or MbS, respectively; fine green arrow – small vesicle inside MbS; fine pink arrows – electron-dense substance on the inner surface of the membranes surrounding MbS. Scale bars 7 µm and 2 µm, respectively.

The latter encompassed the formation of large multi-bacteroids sacs in cells located close to the meristem, gradually (as seen in the developmental sequence, basipetally from the nodule meristem) replacing the typical single-bacteroid symbiosomes. Sac structures were observed previously in genistean cylindrical nodules, but there were only few per cell and they appeared in older zones (Łotocka, 2008). Additionally, in the present study, wall enclaves overgrown into massive and branched structures containing numerous rhizobia were observed and, atypically, these enclaves did not prevent the release of rhizobia within functional BT cells. Normally, in infected cells, rhizobia escape wall enclaves as late as after completion of host's symplast degradation, which results in formation of the saprotrophic zone (Timmers et al., 2000) of the genistean nodules, where small colonies of rod-shaped rhizobia embedded in a polysaccharidic matrix are formed (Łotocka, 2008; Skawińska et al., 2017); these rhizobia live saprotrophically in the dead cell's apoplast and return to soil after final nodule decomposition. However, the most striking developmental disturbance was the formation of discontinuities in the cell walls, which occurred close to the massive wall enclaves, resulting in formation of small syncytia. It strongly resembled the developmental defects discovered in yellow lupine root nodules induced by rhizobia defective in *nodZ* or *nolL* gene functions (Łotocka et al., 2000). The mutations in *nodZ* or *nolL* genes resulted in production of a mixture of incorrect Nod factors ineffective in the molecular dialogue with the host plant. Based on this similarity, it is inferred that rhizobia in the filtrate obtained in the present study from the soil under *L. anagyroides* trees also produced Nod factors incorrectly recognized by the seedlings of this species. However, the reaction of the lupine in the cited study and *L. anagyroides* in the present analys is was different: in lupine, the BT cells gradually gained a normal phenotype, as the MbS gradually fragmented into normal symbiosomes, and the reverse occurred in *L. anagyroides* – the MbS became gradually larger. Moreover, some BT cells entered degradation prematurely in *L. anagyroides* – even in the differentiating zone.

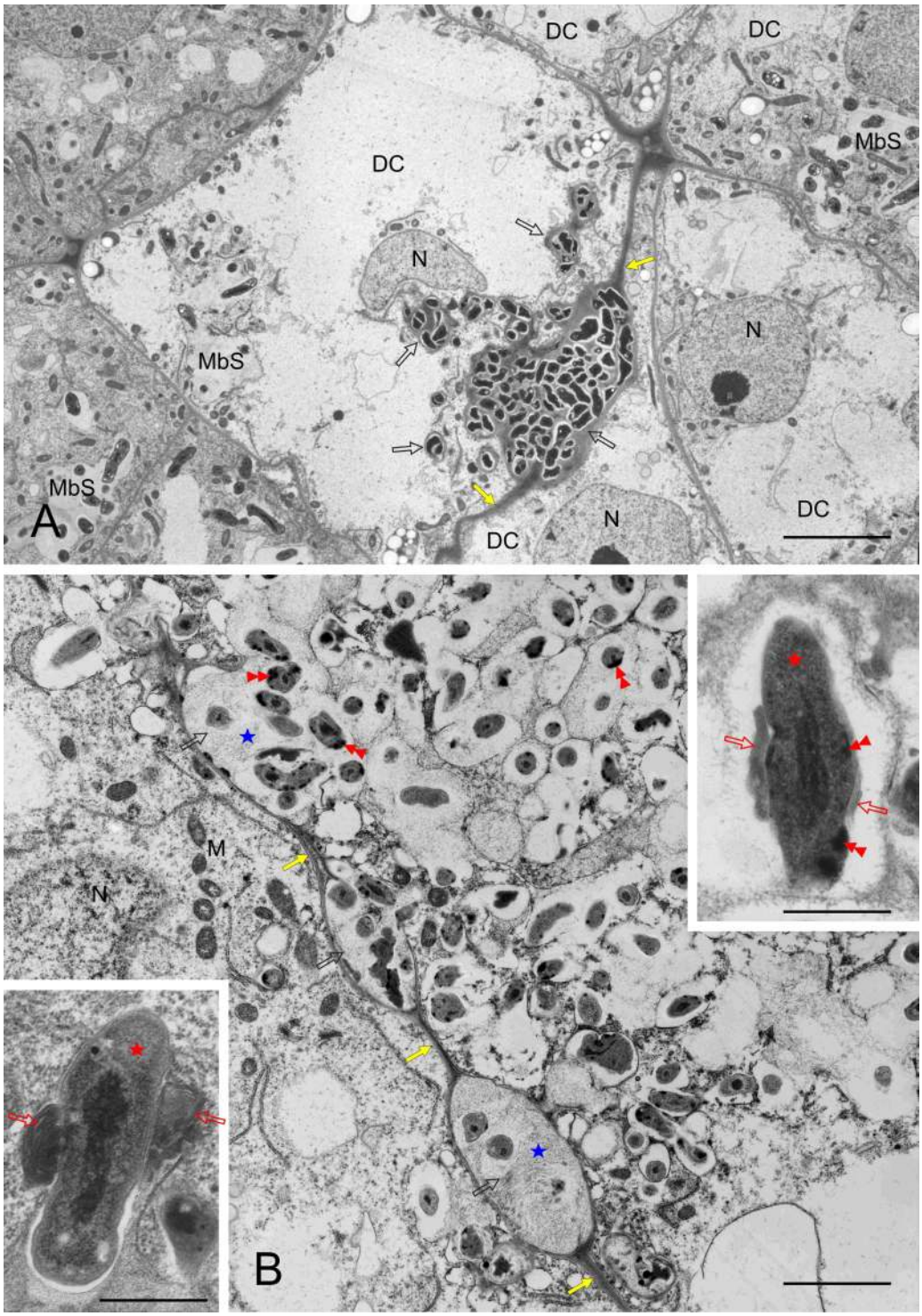

Figure 8 Ultrastructure of clusters of BT cells undergoing degradation, differentiating and differentiated zones in (**A**) and (**B**), respectively. DC – BT cells undergoing degradation; M - mitochondria; MbS – multibacteroid sacs; N – cell nucleus; yellow arrows – cell walls separating BT cells; empty black arrows – cell wall enclaves; blue asterisks - enclave matrix; red asterisks – bacteroids; red double arrowheads – electron dense substance at the periphery of bacteroid cells; empty red arrows – multiseriate membranes or membrane coils at the bacteroid cells. Scale bars 25 µm and 6 µm, respectively, left insert 1 µm, right insert 2 µm.

All the above suggests incompatibility of rhizobia and the host *L. anagyroides* plant, and together with the poor growth and chlorosis, it portraits an ineffective symbiosis. This raises two questions: are the genistean rhizobia compatible with *L. anagyroides* and are there compatible rhizobia available for *L. anagyroides* trees under cultivation in Polish soils? It is generally accepted that rhizobia infecting genisteans belong to the same cross-inoculation group (see the Introduction), and this was the case in previous

studies by the author (review in Łotocka, 2008). Therefore, the assumption that they would nodulate *L. anagyroides* was justified. However, none of the strains fully effective with the native genistean species and lupine were able to induce any nodules in *L. anagyroides* in this study. It was not possible to identify the filtrate-contained rhizobia that nodulated *L. anagyroides* - albeit ineffectively – in this study, but in a different analysis of strains isolated from *L. anagyroides* in Poland, rhizobia compatible with the species were discovered (Sajnaga & Jach, 2020). Among 18 effective strains, three evolutionary lineages were determined that belonged to the *Bradyrhizobium jicamae* supergroup, symbiovar retamae, with *Bradyrhizobium algeriense* and *Bradyrhizobium valentinum* as the closest relatives. However, in an earlier study conducted within the geographical range of *L. anagyroides*, its Spanish microsymbionts were identified as *Bradyrhizobium canariense* (Ruiz-Díez et al., 2009). Significantly, five of rhizobial strains obtained by Sajnaga and Jach (2020) were isolated from *L. anagyroides* grown in a botanical garden, i.e., in a place where numerous foreign species are cultivated for a long time, and therefore the soil microbiome is, most probably, much more modified and richer than typically. All strains were isolated from locations in Lublin and Sandomierz, which differ in soils and weather conditions from Central Poland. Therefore, it is feasible that, in Central Poland, i.e., well-outside the natural range of *L. anagyroides*, the trees do not always meet the compatible rhizobial strains in the typical places where they are planted (private gardens and open green areas), and which, additionally, are often anthropogenically disturbed in urban sites. Significantly, these trees do not reach the "handbook" height (up to 7 m), as noticed by the author, which suggests suboptimal growth conditions in public parks or private gardens. Therefore, the results of the present study indicate a need for a wider survey of the occurrence of compatible strains and, possibly, implementation of effective strains as a commercial *L. anagyroides* inoculum to help nurseries produce trees that would perform better after leaving the nursery.

5. Conclusion

In the present study, the ability of cross-inoculation and effective nodulation by rhizobial microsymbionts effective on other genistean species was not confirmed in *L. anagyroides*. However, the microscopic structure of the nodules induced by a filtrate prepared from soil sampled under established *L. anagyroides* trees met the basic criteria of genistoid nodules. The developmental disturbances detected in the nodules and seedling habit were suggestive of incorrect recognition by the host of the microsymbiont used in the present study.

In juxtaposition with the successful isolation of effective strains in another region of Poland, a hypothesis is made that the availability of compatible microsymbionts is limited in Poland, which is beyond the geographical range of the host species.

Acknowledgments

The Author thanks Ewa Znojek for expert preparation of ultra-thin sections for TEM examinations and anonymous Reviewers for their constructive opinion.

References

Bryan, J. A., Berlyn, G. P., & Gordon, J. C. (1996). Toward a new concept of the evolution of symbiotic nitrogen fixation in the Leguminosae. *Plant and Soil*, *186*, 151–159. https://doi.org/10.1007/BF00035069

Cardoso, D. B. O. S., Pennington, R. T., De Queiroz, L. P., Boatwright, J. S., van Wyk, B. E., Wojciechowski, M. F., & Lavin, M. (2013). Reconstructing the deep-branching relationships of the papilionoid legumes. *South African Journal of Botany*, *89*, 58–75. https://doi.org/10.1016/j.sajb.2013.05.001

Cristofolini, G., & Chiapella, L. F. (1984). Origin and diversification of «Genisteae» (Fabaceae): A serosystematic purview. *Webbia*, *38*(1), 105–122. https://doi.org/10.1080/00837792.1984.10670302

Cristofolini, G., & Conte, L. (2002). Phylogenetic patterns and endemism genesis in *Cytisus* Desf. (Leguminosae-Cytiseae) and related genera. *Israel Journal of Plant Sciences*, *50*(1), 37–50. https://doi.org/10.1560/THU1-K19D-J9GD-7TKH

Golinowski, W., Kopcińska, J., & Borucki, W. (1987). The morphogenesis of lupine root nodules during infection by *Rhizobium lupini*. *Acta Societatis Botanicorum Poloniae*, *56*(4), 687–703. https://doi.org/10.5586/asbp.1987.058

Kalita, M., Stępkowski, T., Łotocka, B., & Małek, W. (2006). Phylogeny and nodulation genes and symbiotic properties of *Genista tinctoria* bradyrhizobia. *Archives of Microbiology*, *186*, 87–97. https://doi.org/10.1007/s00203-006-0124-6

Leeson, C. R., & Leeson, T. S. (1970). Staining methods for sections of epon-embedded tissues for light microscopy. *Canadian Journal of Zoology*, *48*(1), 189–191. https://doi.org/10.1139/z70-026

Łotocka, B. (2008). *Anatomia rozwojowa i ultrastruktura brodawek korzeniowych o nieograniczonym wzroście i jej specyfika u roślin z plemienia Genisteae* [Developmental anatomy and ultrastructure of the indeterminate root nodules and their specificity in genisteans]. SGGW.

Łotocka, B., Arciszewska-Kozubowska, B., Dąbrowska, K., & Golinowski, W. (1995). Growth analysis of root nodules in yellow lupin. *Annals of Warsaw Agricultural University - SGGW, Agriculture*, *29*, 3–12.

Łotocka, B., Kopcińska, J., Borucki, W., Stępkowski, T., Świderska, A., Golinowski, W., & Legocki, A. (2000). The effects of mutations in *nolL* and *nodZ* genes of *Bradyrhizobium* sp. WM9 (*Lupinus*) upon root nodule ultrastructure in *Lupinus luteus* L. *Acta Biologica Cracoviensia. Series Botanica*, *42*(1), 155–163.

O'Brien, T. P., Feder, N., & McCully, M. E. (1964). Polychromatic staining of plant cell walls by toluidine blue-O. *Protoplasma*, *59*, 367–373. https://doi.org/10.1007/BF01248568

Polish Nurserymen Association. (2023, July 20). https://zszp.pl

Rivers, M. C. (2017). *Laburnum anagyroides*. *The IUCN Red List of Threatened Species, 2017*, Article e.T79919483A79919650. https://doi.org/10.2305/IUCN.UK.2017-3.RLTS.T79919483A79919650.en

Ruiz-Díez, B., Fajardo, S., Puertas-Mejía, M. A., de Felipe, M. D. R., & Fernández-Pascual, M. (2009). Stress tolerance, genetic analysis and symbiotic properties of root-nodulating bacteria isolated from Mediterranean leguminous shrubs in Central Spain. *Archives of Microbiology*, *191*(1), 35–46. https://doi.org/10.1007/s00203-008-0426-y

Sajnaga, E., & Jach, M. E. (2020). Bradyrhizobia associated with *Laburnum anagyroides*, an exotic legume grown in Poland. *Symbiosis*, *80*, 245–255. https://doi.org/10.1007/s13199-020-00668-x

Sajnaga, E., Małek, W., Łotocka, B., Stępkowski, T., & Legocki, A. (2001). The root-nodule symbiosis between *Sarothamnus scoparius* L. and its microsymbionts. *Antonie van Leeuwenhoek*, *79*(3), 385–391. https://doi.org/10.1023/A:1012010328061

Selami, N., Auriac, M. C., Catrice, O., Capela, D., Kaid-Harche, M., & Timmers, T. (2014). Morphology and anatomy of root nodules of *Retama monosperma* (L.) Boiss. *Plant and Soil*, *379*(1), 109–119. https://doi.org/10.1007/s11104-014-2045-5

Seneta, W., Dolatowski, J., & Zieliński, J. (2021). *Dendrologia* [Dendrology]. PWN.

Skawińska, M., Łotocka, B., Ruszkowski, T., Banaszczak, P., & Znojek, E. (2017). Root nodule structure in *Chamaecytisus podolicus*. *Acta Agrobotanica*, *70*, Article 1716. https://doi.org/10.5586/aa.1716

Stevens, P. F. (2001, onwards). *Angiosperm Phylogeny Website. Version 14, July 2017*. http://www.mobot.org/MOBOT/research/APweb/

Stępkowski, T., Banasiewicz, J., Granada, C. E., Andrews, M., & Passaglia, L. M. (2018). Phylogeny and phylogeography of rhizobial symbionts nodulating legumes of the tribe Genisteae. *Genes*, *9*(3), Article 163. https://doi.org/10.3390/genes9030163

Stępkowski, T., Świderska, A., Miedzińska, K., Czaplińska, M., Świderski, M., Biesiadka, J., & Legocki, A. B. (2003). Low sequence similarity and gene content of symbiotic clusters of *Bradyrhizobium* sp. WM9 (*Lupinus*) indicate early divergence of "lupin" lineage in the genus *Bradyrhizobium*. *Antonie van Leeuwenhoek*, *84*, 115–124. https://doi.org/10.1023/A:1025480418721

Timmers, A. C., Soupène, E., Auriac, M. C., de Billy, F., Vasse, J., Boistard, P., & Truchet, G. (2000). Saprophytic intracellular rhizobia in alfalfa nodules. *Molecular Plant–Microbe Interactions*, *13*, 1204–1213. https://doi.org/10.1094/MPMI.2000.13.11.1204

Tokarska-Guzik, B., Dajdok, Z., Zając, M., Zając, A., Urbisz, A., Danielewicz, W., & Hołdyński, C. (2012). *Rośliny obcego pochodzenia w Polsce ze szczególnym uwzględnieniem gatunków inwazyjnych* [Plants of foreign origin in Poland, with particular emphasis on invasive species]. Generalna Dyrekcja Ochrony Środowiska.

Vincent, J. M. (1970). *A manual for the practical study of the root-nodule bacteria*. JBP Handbook 15, Blackwell Scientific Publications Ltd.

Wysocki, C. (2019). Funkcjonowanie szaty roślinnej w warunkach miejskich [The functioning of plant cover in urban conditions]. *Przegląd Geograficzny*, *91*, 421–434. https://doi.org/10.7163/PrzG.2019.3.7

Zalewska, E. D., Zawiślak, G., & Król, E. D. (2023). Fungi inhabiting aboveground organs of sea buckthorn (*Hippophae rhamnoides* L.) in organic farming. *Acta Agrobotanica*, *76*, Article 174959. https://doi.org/10.5586/aa/168497